4A.4 ESTIMATION OF LOW-LEVEL WIND STURCTURES IN A TORNADO-LIKE VORTEX

Sean Crowell[*†‡], L.J. Wicker[‡] and L.W. White[†]

1. INTRODUCTION

The last few decades have seen major breakthroughs in the understanding of severe storms, resulting both from improved modeling capabilities and observational field work. One remaining frontier is the tornadic vortex, especially a quantitative understanding of the lowest few hundred meters above the ground. Researchers have published many articles (e.g. Bluestein et al (2004), Bluestein et al (2007)) detailing observations of storm and tornado scale features using moderate and fine scale resolution mobile radars. However, mobile radar platforms have failed to observe features near ground level that theoretical considerations imply should exist, such as the corner flow and inflow regions of the tornado. This work outlines a method of estimating wind structures in the absence of data at low levels that assumes a regular structure in the tangential component of the tornado's wind velocity field and simplified dynamics for the wind fields, and shows the results of tests in an observing system simulation experiment (OSSE).

2. SIMPLIFIED DYNAMICS MODEL EQUATIONS

Keeping operational considerations in mind, as well as concerns of mathematical tractability, we opt for a simplified set of equations. This is justified physically by the fact that in the lowest portion of the tornado, it is likely that moisture and temperature fields are much less important than the balance of momentum and mass continuity. Denote by (u, v, w) the radial, tangential, and vertical components of velocity. As an initial approximation, we consider the axisymmetric, steady form of the equations of motion in cylindrical coordinates centered at the vortex center. The tangential momentum and mass continuity equations take the form

$$\zeta u - \eta w = \nu(\zeta_r - \eta_z) \tag{2.1}$$

$$\frac{1}{r}(ru)_r + w_z = 0. \tag{2.2}$$

Our goal here is to estimate v from radar data, and then estimate u and w using these equations. The domain on which we consider this problem is a rectangle in the $r-z$ plane. The upper boundary of this domain is the minimum observable height h, likely to be a few hundred meters for mobile radar platforms, and so data along this "lid" can be taken as a boundary condition. We will see that for points on the interior of the domain, knowledge of the other boundary conditions is unnecessary, as the top boundary's information propagates into the domain along characteristic curves.

3. SOLUTION BY METHOD OF CHARACTERISTICS

By solving (2.1) for u or w and substituting the result into (2.2), we end up with one of the following two sets of characteristic equations

$$\frac{dr}{dt} = \eta \tag{3.1}$$

$$\frac{dz}{dt} = \zeta \tag{3.2}$$

$$\frac{dw}{dt} + \frac{\zeta}{r}\left(r\frac{\eta}{\zeta}\right)_r w = -\frac{\nu\zeta}{r}\left(r\frac{\zeta_r - \eta_z}{\zeta}\right)_r \tag{3.3}$$

if we solve for u and

$$\frac{dr}{dt} = \eta \tag{3.4}$$

$$\frac{dz}{dt} = \zeta \tag{3.5}$$

$$\frac{du}{dt} + \left(\frac{\eta}{r} + \eta\frac{\partial}{\partial z}\frac{\zeta}{\eta}\right)u = \nu\eta\frac{\partial}{\partial z}\frac{\zeta_r - \eta_z}{\eta} \tag{3.6}$$

[*]Corresponding Author: scrowell@ou.edu
[†]Department of Mathematics, University of Oklahoma
[‡]National Severe Storms Laboratory

if we solve for w. Note that the characteristic curves $(r(t), z(t))$ are the same for both sets of equations. This is useful, because it means that the relations for u and w hold on the same "time" scale. Here we take our initial conditions to be the velocities on the lid.

It is possible that ζ or η could be zero at values of r or z inside Ω. When this happens, the characteristic ordinary differential equations are singular. However, if v is known, we can diagnose u (if $\zeta \neq 0$) or w (if $\eta \neq 0$) and then find the other component from the mass continuity equation.

4. WOOD-WHITE MODEL

We take $v(r,z) = v_{\max}\phi(r)\psi(z)$, where ϕ is estimated from data, and ψ is taken to model the tangential wind fields below the observable height. The functional form for ϕ (and ψ for the Davies-Jones dataset) is given by

$$\phi(r; n, k, R) = \frac{nR^{n-k}r^k}{(n-k)R^n + kr^n}. \tag{4.1}$$

Here n and k are shape parameters for the Woods-White tangential velocity, and R is the radius of maximum wind speed. This model is a smooth function that generalizes the Rankine vortex model

$$v_{rk}(r) = \begin{cases} v_{\max}r/R & r \leq R \\ v_{\max}R/r & r \geq R \end{cases} \tag{4.2}$$

that is commonly used in wind field estimation. It shares a few properties with the Rankine vortex model, namely that the velocity is equal to $v_{\max}$ at $r = R$, the slope is positive for $r < R$ and negative for $r > R$. There is more flexibility in the shape, which lends itself well to data fitting.

Note that

$$\zeta(r,z) = v_{\max}\left(\frac{1}{r}\frac{d}{dr}(r\phi(r;n,k,R))\right)_r \psi(z),$$

and expanding $\left(\frac{1}{r}\frac{d}{dr}(r\phi(r;n,k,R))\right)_r$, we get

$$\frac{1}{r}\frac{d}{dr}(r\phi(r;n,k,R)) = \frac{nr^{k-1}R^{n-k}}{((n-k)R^n + kr^n)^2} \tag{4.3}$$
$$\left((k^2 - k(n-1))r^n + (n + k^2 - k(n-1))R^n\right)$$

implying $\zeta = 0$ when $r = 0$ if $k \neq 1$. This forces $u(0,z) = \pm\infty$ when $k \neq 1$. Thus, we will require $k = 1$, which reduces the parameter space dimension by one.

5. CHARACTERISTIC METHOD WITH WOOD-WHITE MODEL

Following Snow (1982), the vertical variation $\psi(z)$ in the tangential wind field in the lowest vertical levels of the tornado can be modeled by the function (4.1), with the same caveat about forcing $k = 1$, only this time so that w will be finite at $z = 0$, and of course choosing a different n parameter. Hence, let

$$v(r,z) = v_{\max}\phi(r; n_r, R)\phi(z; n_z, Z) \tag{5.1}$$

$$\zeta(r,z) = v_{\max}\frac{1}{r}\frac{d}{dr}(r\phi(r; n_r, R))\phi(z; n_z, Z) \tag{5.2}$$

$$\eta(r,z) = -v_{\max}\phi(r; n_r, R)\frac{d}{dz}\phi(z; n_z, Z) \tag{5.3}$$

In the next sections, I will detail how the characteristic curves and solutions u and w behave with this as our ansatz.

5.1 *Characteristic Curves*

From (3.1) and (3.2), we see that r follows the sign of η and z follows the sign of ζ. This leads to a couple of immediate results. First, the vertical axis is a characteristic curve because $\eta = 0$ when $r = 0$. Similarly, the polar axis is also a characteristic curve. Note that η is negative for $z < Z$ and positive for $z > Z$, while ζ is positive for $r < R_\zeta$ and negative for $r > R_\zeta$, where

$$R_\zeta = \left(\frac{2(n-1)}{n-2}\right)^{1/n} R. \tag{5.4}$$

This divides Ω into four regions, with the behavior of the characteristic curves depending on which region the curve is passing through. Figure 1(a) is a schematic drawing of the behavior of the characteristic curves. The arrows are pointing in the direction that the values of $(r(t), z(t))$ move as t increases. The question of existence of unique solutions is automatically answered from these inequalities. We know that the characteristic curves won't cross, because they're the level curves of $\Gamma = rv(r,z)$, which is a continuously differentiable function on Ω. Hence, if (r,z) is a point in Ω, there will be an r_0 so that the characteristic passing through (r_0, h) also passes through (r,z).

5.2 *Inviscid Case ($\nu = 0$)*

Examining the integrating factor solution of (3.3), we can determine the regions of Ω where w is increasing and decreasing. Initially, assume $\nu = 0$, so that the solution reduces to

$$w(t) = w(0) \exp\left(-\int_0^t \zeta \left(\frac{\eta}{\zeta} \right)_r ds \right). \qquad (5.5)$$

By writing out the integrand explicitly in terms of the component models, we have

$$\frac{1}{\zeta}\left(\eta_r \zeta - \eta \zeta_r\right) = \frac{\phi_z(z)}{\frac{1}{r}(r\phi(r))_r} \times \qquad (5.6)$$
$$\left(r\phi(r) \left(\frac{1}{r}(r\phi(r))_r \right)_r - \frac{\phi_r(r)}{r}(r\phi(r))_r \right)$$

The quantity in parentheses is zero when

$$r = R_w := R \left(\frac{n_r - 1}{2(n_r - 2)} \right)^{1/n_r} \times \qquad (5.7)$$
$$\left(n_r^2 - n_r + 1 \pm n_r \sqrt{n_r^2 - 2n_r + 8} \right)^{1/n_r}$$

The quantity after the $\pm$ is bigger than that in front, so the second zero would be negative, and hence is not of any interest to us. From the equation that we used to derive the value R_w we find that the quantity in parentheses in (5.6) is negative to the left of R_w and positive to the right of R_w. We already know where the other two factors in (5.6) change sign. This leads to the sign chart in Figure 1(b), and tells us where w is increasing and decreasing.

6. PROBABILISTIC ESTIMATION

For a set of observed values tangential winds, we can define a cost functional by

$$J(\vec{q}) = \frac{1}{2} \sum_{obs} \left(v_{\max} \phi(r; \vec{q}_r) \psi(z; \vec{q}_z) - \hat{v}_i \right)^2, \qquad (6.1)$$

where $\vec{q} = [v_{\max}, \vec{q}_r, \vec{q}_z]$. Following Tarantola (2005), we can define a probability density function $p(\vec{q})$ over the parameter space by

$$p(\vec{q}) = \kappa e^{-J} \qquad (6.2)$$

with κ chosen as a normalizing constant. From this vantage point, we can view the optimal parameter values which minimize J, i.e. the least-squares values of $\vec{q}$ as the maximum likelihood estimate (MLE) for p. Taking into account the fact that our model is a simplified version of reality, we can view sampling p as accounting for uncertainties in the model and the data. With some caveats, we can use p to bring the ideas of information theory to bear on the problem of estimating v. Further, the probabilistic method of estimating v leads to distributions of u and w, for which we can calculate statistics.

7. TESTS WITH DAVIES-JONES' MODEL OUTPUT

In Davies-Jones (2008), Davies-Jones describes an unsteady axisymmetric storm- and tornado-scale model, with the intention of determining the role of precipitation in tornadogenesis. As a part of our Observing System Simulation Experiment (OSSE), we used a single snapshot (in time) from the output of this model that produced a tornado cyclone as data, with the goal of estimating the wind fields near the ground.

7.1 *Parameters*

We sampled (6.2) with v of the form in (5.1), choosing the parameters that have the largest *likelihood*, which is the value of p at a chosen parameter vector for a particular set of data. We used various values for the minimum observable height h, chosen to agree with the vertical levels in the data. In the model, Davies-Jones used a value of 0.0005 for ν, so our inviscid special case described above is applicable here.

7.2 *Experiments*

For these tests, I used the Davies-Jones model grid as the points where I estimated the radial and vertical velocities, for comparison with the true values in an ℓ_2 sense. Figure 1 show the qualitative properties of the inviscid solution w from the properties of ζ and η in specified regions of the domain. The simplest estimate would be the u and w coming from the maximum likelihood estimate of v. Another estimate would be a sample conditional mean, computed by sampling the pdf at the most likely parameter vectors. These comparisons are shown in Figure 2 and 3 for a minimum observable height of 462 meters. Table 1 and 2 show the objective error values for four different minimum observable heights. Note that while the contour plots look similar, there is a striking difference in the objective error measurements, with the mean fields usually being more accurate than the MLE fields.

7.3 *Numerical Integration*

The equations were integrated using various numerical methods, and showed little sensitivity to choice of method for appropriate time step sizes. The results shown use an implicit Euler method, chosen for its simplicity and stability properties. Loosely speaking, this method was the optimal one for balancing integration time with accuracy. Higher order methods were explored, but did not seem to give enough improvement to warrant the cost. The equations were integrated on an eight-core Intel Power Mac.

7.4 *Caveats*

These experiments assume knowledge of all of the wind components above the observable height h. This is an unrealistic assumption, as we really only measure a single Doppler velocity that contains almost no information about the vertical velocity. Estimating vertical velocities from radar measurements is an active area of research. When I attempted to use (2.1) to get the w initial condition from u, which is physically more reasonable, the results were seriously degraded. Any attempt to move forward from here will have to include a more realistic method of estimating w from the two horizontal wind components, in order to give initial conditions for the characteristic equations.

Another physical issue is the meaning of the constant ν. Steady flow will be much less sensitive to this constant than if we allowed unsteady flow, where ν would govern removal of energy from the system by turbulent or diffusive processes. A more realistic problem will have to provide some estimate for ν, and may need to provide for the possibility that ν won't be spatially constant, but rather flow dependent.

8. References

Bluestein, H., C. Weiss and A. Pazmany. Vertical Structure of a Tornado near Happy, Texas, on 5 May 2002: High-Resolution, Mobile, W-Band, Doppler Radar Observations. *Mon Wea Rev* 132, 2325-2337. 2004.

Bluestein, H., C. Weiss, M. French, C. Holthaus, and R. Tanamachi. The Structure of Tornadoes near Attica, Kansas, on 12 May 2004: High Resolution, Mobile, Doppler Radar Observations. *Mon Wea Rev* 135, 475-506. 2007.

Davies-Jones, R. Can a Descending Rain Curtain in a Supercell Instigate Tornadogenesis Barotropically? *J Atmos Sci* 65, 2469-2497. 2008.

Snow, J. A Review of Recent Advances in Tornado Vortex Dynamics. *Rev Geophys Space Phys* 20(4), 953-964. 1982.

Tarantola, A. Inverse Problem Theory and Methods for Model Parameter Estimation. SIAM, 2005.

Root Mean Square Error				
h	MLE U	Mean U	MLE W	Mean W
294	5.74	4.23	2.73	2.56
462	6.43	4.12	3.77	3.77
630	6.50	4.11	3.84	5.23
798	9.26	4.56	5.09	3.53

Table 1: Root Mean Square errors in estimates of the radial and vertical wind components as functions of the minimum observable height h.

Maximum Absolute Error				
h	MLE U	Mean U	MLE W	Mean W
294	12.64	10.24	6.05	5.09
462	14.34	9.75	8.56	8.43
630	14.14	8.82	9.14	15.43
798	18.40	10.42	11.60	8.20

Table 2: Maximum errors in estimates of the radial and vertical wind components as functions of the minimum observable height h.

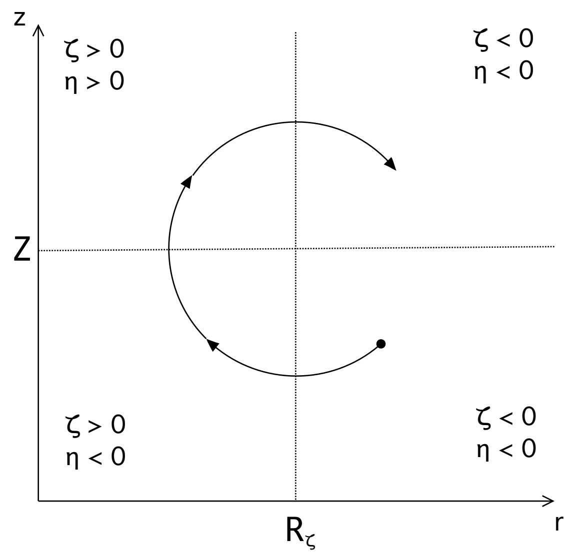

(a) Schematic of Characteristic Curves

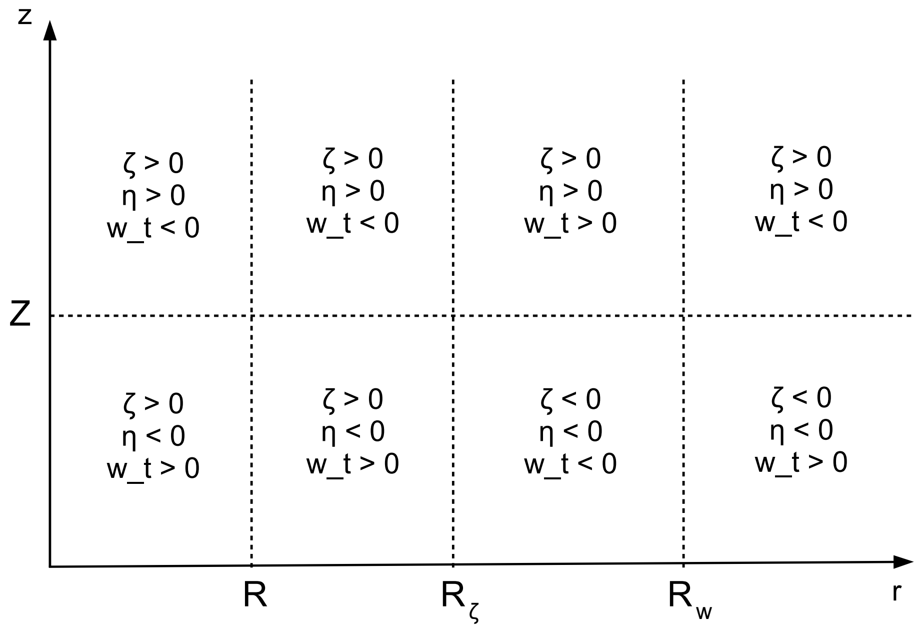

(b) Sign of $\frac{dw}{dt}$ with $\nu = 0$

Figure 1: (a) Characteristic curve schematic and (b) Sign of $\frac{dw}{dt}$ with $\nu = 0$ associated to the tangential velocity $v = v_{\max}\phi(r)\phi(z)$

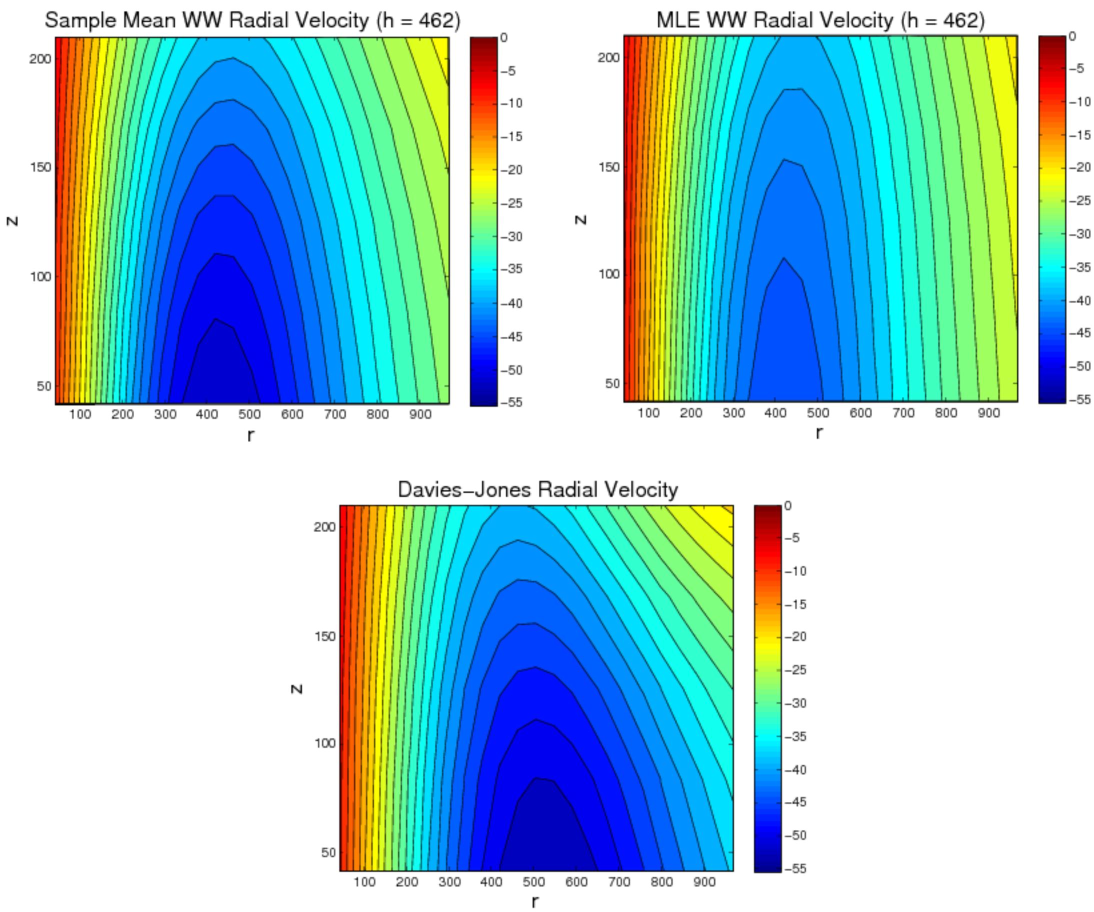

Figure 2: Comparison of Sample Mean and MLE estimates for u with Davies-Jones u, when $h = 462$m.

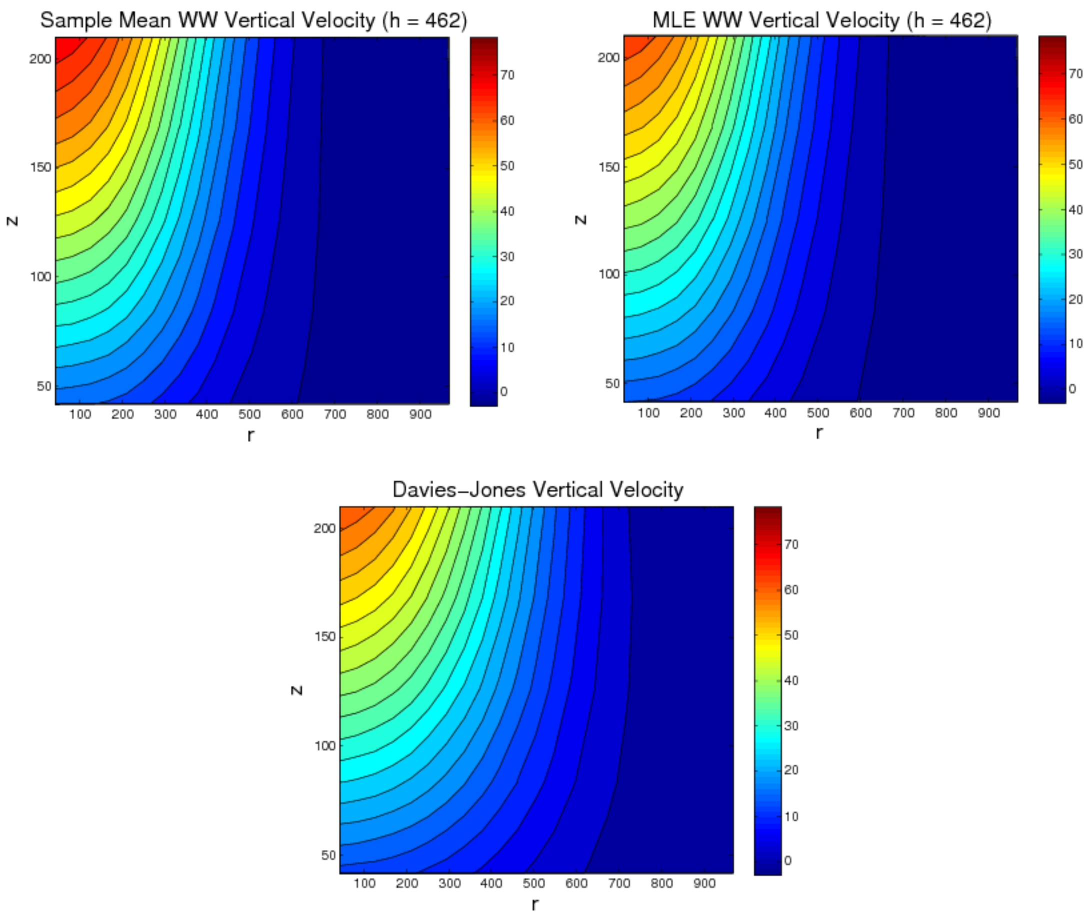

Figure 3: Comparison of Sample Mean and MLE estimates for u with Davies-Jones u, when $h = 462$m.